

Effective dynamics of the Schwarzschild black hole interior with inverse triad corrections

Hugo A. Morales-Técotl,^{1,2,*} Saeed Rastgoo,^{3,1,4,†} and Juan C. Ruelas^{1,‡}

¹*Departamento de Física, Universidad Autónoma Metropolitana - Iztapalapa
San Rafael Atlixco 186, Ciudad de Mexico 09340, Mexico*

²*Departamento de Física, Escuela Superior de Física
y Matemáticas del Instituto Politécnico Nacional
Unidad Adolfo López Mateos, Edificio 9, 07738 Ciudad de México, Mexico*

³*School of Sciences and Engineering
Monterrey Institute of Technology (ITESM), Campus León
Av. Eugenio Garza Sada, León, Guanajuato 37190, Mexico*

⁴*Department of Physics and Astronomy,
York University 4700 Keele Street, Toronto, Ontario M3J 1P3, Canada*

(Dated: January 22, 2021)

We reconsider the study of the interior of the Schwarzschild black hole now including inverse triad quantum corrections within loop quantization. We derive these corrections and show that they are related to two parameters δ_b, δ_c associated to the minimum length in the radial and angular directions, that enter Thiemann's trick for quantum inverse triads. Introduction of such corrections may lead to non-invariance of physical results under rescaling of the fiducial volume needed to compute the dynamics, due to noncompact topology of the model. So, we put forward two prescriptions to resolve this issue. These prescriptions amount to interchange δ_b, δ_c in classical computations in Thiemann's trick. By implementing the inverse triad corrections we found, previous results such as singularity resolution and black-to-white hole bounce hold with different values for the minimum radius-at-bounce, and the mass of the white hole.

I. INTRODUCTION

As one of the most fascinating predictions of general relativity, black holes have been the subject of much analysis and explorations. Particularly their interior, and the singularity located there, has been studied in classical, quantum and semiclassical regimes. The mainstream hope is that the classical singularity will be resolved and replaced by a quantum region. However, there are still many open issues to be answered in a satisfactory way. Within loop quantum gravity (LQG) [1, 2], there have been numerous works about quantum black holes and their singularity resolution in both mini- and midi-superspace models, to mention a few [3–15]. One of the most studied models in this context is the Schwarzschild black hole which interior corresponds to a Kantowski-Sachs model, a system with finite degrees of freedom, and hence a mini-superspace, with a singularity at the heart of it [4, 16]. One of the approaches to quantize this model, inspired by LQG, is polymer quantization

* hugo@xanum.uam.mx

† srastgoo@yorku.ca

‡ carlos.ruelas@tec.mx

[17–20], a technique also used in loop quantum cosmology (LQC) [21–23]. In this quantization the classical canonical algebra is represented in a way that is unitarily inequivalent to the usual Schrödinger representation even at the kinematical level. The root of this inequivalency is the choice of topology and the form of the inner product of this representation, which renders some of the operators discontinuous in their parameters, resulting in the representation not being weakly continuous. On the other hand, unitary equivalency of a representation to the Schrödinger one is guaranteed by the Stone-von Neumann theorem iff all of its premises, including weak continuity of the representation, are satisfied, and the polymer representation does not. This inequivalency translates into new results that are different from the usual quantization of the system, one of them being the resolution of the singularity of the Kantowski-Sachs model. These results however, are accompanied by some issues that we briefly discuss in what follows.

In one of the earliest attempts in this approach [3], the authors showed that the singularity can be avoided in the quantum regime, but one of the important issues was the dependence of results on auxiliary parameters that define the size of the fiducial cell. The introduction of this fiducial cell, in this case a cylindrical one with topology $\mathcal{I} \times \mathbb{S}^2$ and volume $V_0 = a_0 L_0$, where a_0 is the area of the 2-sphere \mathbb{S}^2 and L_0 is the cylinder’s height, is necessary to avoid the divergence of some of the spatial integrals in homogenous models with some non-compact directions. Particularly it is important to be able to define the symplectic structure. Given that the physical results should not depend on these auxiliary parameters, a new proposal, motivated by the “improved quantization” in LQC [24], was put forward that avoided this dependence and yielded bounded expansion and shear scalars [4]. However, this method also leads to some undesired modified behavior at the horizon due to quantum gravitational effects in vacuum, that are manifestation of the coordinate singularity there. There are also some other recent works that take a bit of a different approach to the problem by looking for an effective metric [25, 26].

In [6], a key modification to the quantization was proposed by choosing to fix $a_0 := 4\pi r_0^2$ by a physical scale r_0 . This physical r_0 permits one to define a Hamiltonian formulation, and in this way is different in nature from the auxiliary scale L_0 , which is needed to fix the fiducial cell size to be able to define the symplectic structure. Thus while r_0 will be present in physical results in both the classical and quantum theories, these theories should be independent of L_0 . The proposal in [6], leads to results that are independent of the auxiliary parameters, and while the theory predicts that the singularity is resolved in the quantum gravity regime, no large quantum gravitational effects appear at low curvatures near the horizon as it should be the case.

It is worth noting that the anisotropic models suffered from an issue: since these models resolve the singularity, they predicted a “bounce” from a black hole to a white hole, with the mass M_W of the resultant white hole not matching with that of the original black hole $M_B \neq M_W$, but rather $M_W \propto M_B^4$. Recent work presented some proposals to deal with it [27] and a different approach was developed in [28, 29] by encompassing the interior region containing the classical singularity with the exterior asymptotic one, which, in the large mass limit, makes the masses of the white and black holes take the same value. See also [30–32] for a different perspective.

All previous works on black holes ignore inverse triad corrections, to simplify the problem. However, they are important especially at highly quantum regimes and a more complete quantum gravitational analysis of this model should take them into account. In this work we first use a path integral in phase space including inverse triad quantum corrections.

These corrections are known to produce severe issues in non compact cosmological models, among them the dependence of the physical quantities on the auxiliary parameters or their rescaling. We put forward two proposals that, in the case of Schwarzschild black hole, yield a physical description with no reference to fiducial parameters. Finally, we study how these proposals modify the “minimum radius at the bounce”.

The structure of this paper is as follows: In section II, we present the background, the relation between the Schwarzschild interior and the Kantowski-Sachs model, and their classical Hamiltonian analysis. In section III, we briefly review how the quantum Hamiltonian constraint is defined. In section IV, the path integral analysis is presented and it is shown how a systematic effective Hamiltonian constraint can be derived from the quantum Hamiltonian, including inverse triad corrections. Section V is dedicated to presenting some of the important issues that are raised by the presence of the new corrections, and recognizing the root of these issues. In section VI, we present two proposals to deal with the aforementioned issues, and also show their effect upon some physical quantities. Finally, in section VII, we conclude the paper by presenting a summary and a discussion about the results.

II. BACKGROUND AND THE CLASSICAL THEORY

For Schwarzschild black hole the spacetime metric

$$ds^2 = - \left(1 - \frac{2GM}{r}\right) dt^2 + \left(1 - \frac{2GM}{r}\right)^{-1} dr^2 + r^2 (d\theta^2 + \sin^2 \theta d\phi^2) \quad (2.1)$$

where M is the mass of the black hole, the timelike and spacelike curves switch their causal nature into each other for observers that cross the event horizon. Hence the metric of the interior region is obtained by $r \leftrightarrow t$,

$$ds^2 = - \left(\frac{2GM}{t} - 1\right)^{-1} dt^2 + \left(\frac{2GM}{t} - 1\right) dr^2 + t^2 (d\theta^2 + \sin^2 \theta d\phi^2), \quad (2.2)$$

with $t \in (0, 2GM)$ and $r \in (-\infty, \infty)$. This metric is a special case of a Kantowski-Sachs cosmological spacetime that is given by the metric

$$ds^2 = -d\tau^2 + A^2(\tau)dr^2 + B^2(\tau) (d\theta^2 + \sin^2 \theta d\phi^2). \quad (2.3)$$

The coordinates in which (2.3) is written are Gaussian normal coordinates adapted to the comoving observers, *i.e.*, the time coordinate curves are the worldlines of the free falling objects (*e.g.* stars) that are at rest with respect to such observers, and are parametrized by their proper time τ . The metric (2.2) can be seen to be derived from (2.3) by the transformation

$$d\tau^2 = \left(\frac{2GM}{t} - 1\right)^{-1} dt^2. \quad (2.4)$$

Choosing positive root of the above, we get

$$\tau = -\sqrt{t(2GM - t)} - GM \tan^{-1} \left(\frac{t - GM}{\sqrt{t(2GM - t)}} \right) + \frac{GM\pi}{2}, \quad (2.5)$$

where the last term in the right hand side is the integration constant and it is chosen such that $\tau \rightarrow 0$ for $t \rightarrow 0$ (at singularity), and $\tau \rightarrow GM\pi$ for $t \rightarrow 2GM$ (at the horizon), hence $\tau \in (0, GM\pi)$. Then τ is a monotonic function of t . Written in Gaussian normal coordinates (τ, r, θ, ϕ) , the Schwarzschild metric takes the form (2.3), with $A^2(\tau) = \frac{2GM}{t(\tau)} - 1$ and $B^2(\tau) = \tau^2$.

The Kantowski-Sachs metric (2.3) in general and the Schwarzschild interior (2.2) in particular, represent a spacetime with spatial homogeneous but anisotropic foliations; one can consider $A(\tau)$ and $B(\tau)$ as two distinct scale factors that affect the radial and angular parts of the metric separately. Thus the interior region is a model with no local degrees of freedom, *i.e.*, it can be described as a mechanical system with a finite number of configuration variables. In gravitational language, this corresponds to a mini-superspace model. From the computational point of view, this is an important property that is exploited in quantizing the Schwarzschild interior as we will see.

It also can be seen from the metric (2.3) and (2.2), that the spacetime is foliated such that the spatial hypersurfaces have topology $\mathbb{R} \times \mathbb{S}^2$, and the symmetry group is the Kantowski-Sachs isometry group $\mathbb{R} \times SO(3)$. The aforementioned topology of the model means that there exists one noncompact direction, $r \in \mathbb{R}$ in space. Thus in order to be able to compute quantities that involve integrals over space, particularly the symplectic structure $\int_{\mathbb{R} \times \mathbb{S}^2} d^3x dq \wedge dp$, one needs to choose a finite fiducial volume over which these integrals are calculated, otherwise the integrals will diverge. This is a common practice in the study of homogeneous minisuperspace models, which here, is done by introducing an auxiliary length L_0 to restrict the noncompact direction to an interval $r \in \mathcal{I} = [0, L_0]$. The volume of the fiducial cylindrical cell in this case is $V_0 = a_0 L_0$, where a_0 is the area of the 2-sphere \mathbb{S}^2 in $\mathcal{I} \times \mathbb{S}^2$. Now, for the area a_0 , there are at least two choices: One can use it as an auxiliary parameter, or fix it using a physical scale. In any case, the final physical results should not depend on the choice of auxiliary parameters. In a recent work [6], a choice has been put forward, in which the \mathbb{S}^2 area of the fiducial volume is fixed to be $a_0 := 4\pi r_0^2$ where r_0 is a physical scale that is identified with the Schwarzschild radius. This choice can be considered as a boundary condition which ensures that the classical limit becomes the classical Schwarzschild solution with radius r_0 . Using this choice, the volume of the cylindrical fiducial cell becomes $V_0 = 4\pi r_0^2 L_0$, and the associated fiducial metric is denoted by ${}^0q_{ab}$. Using a physical scale for a_0 , instead of an auxiliary nonphysical one, seems to be a key ingredient that fixes some of the issues with previous attempts at loop quantization of the interior of Schwarzschild black hole, and here we follow this choice.

The starting point of the Hamiltonian analysis in this approach is to write down the classical configuration variable, the $su(2)$ Ashtekar-Barbero connection A_a^i , and its conjugate momentum, the desitized triad E_i^a , in the relevant coordinate basis. Given the symmetries of this spacetime and after imposing the Gauss constraint, these variables take the form [3, 6]

$$A_a^i \tau_i dx^a = \bar{c} \tau_3 dr + \bar{b} r_0 \tau_2 d\theta - \bar{b} r_0 \tau_1 \sin \theta d\phi + \tau_3 \cos \theta d\phi, \quad (2.6)$$

$$E_i^a \tau^i \frac{\partial}{\partial x^a} = \bar{p}_c r_0^2 \tau_3 \sin \theta \frac{\partial}{\partial r} + \bar{p}_b r_0 \tau_2 \sin \theta \frac{\partial}{\partial \theta} - \bar{p}_b r_0 \tau_1 \frac{\partial}{\partial \phi}, \quad (2.7)$$

where \bar{b} , \bar{c} , \bar{p}_b and \bar{p}_c are functions that only depend on time t , and $\tau_i = -i\sigma_i/2$ are a $su(2)$ basis with σ_i being the Pauli matrices. $r_0 = 2GM$ is the Schwarzschild radius. In these

variables the Schwarzschild interior metric becomes

$$ds^2 = -N^2 dt^2 + \frac{\bar{p}_b^2}{\bar{p}_c} dr^2 + \bar{p}_c r_0^2 (d\theta^2 + \sin^2 \theta d\phi^2), \quad (2.8)$$

where we have chosen $\bar{p}_c \geq 0$ given that it is related to the radial coordinate (see below). Now, the symplectic structure can be computed by performing an integration over the fiducial volume as

$$\begin{aligned} \Xi &= \frac{1}{8\pi G\gamma} \int_{\mathcal{I} \times S^2} d^3x \quad dA_a^i \wedge dE_i^a \\ &= \frac{L_0 r_0^2}{2G\gamma} (d\bar{c} \wedge d\bar{p}_c + 2d\bar{b} \wedge d\bar{p}_b), \end{aligned} \quad (2.9)$$

where γ is the Barbero-Immirzi parameter [1]. Clearly, in these variables, the symplectic structure and thus the Poisson algebra depends on L_0 . To remove this dependency, it is customary to redefine the variables in the following way

$$c = L_0 \bar{c}, \quad p_c = r_0^2 \bar{p}_c \quad b = r_0 \bar{b} \quad p_b = r_0 L_0 \bar{p}_b. \quad (2.10)$$

As a result the Poisson algebra between these redefined variables, and other *physical* quantities are explicitly independent of the auxiliary variable L_0 ,

$$\{c, p_c\} = 2G\gamma, \quad \{b, p_b\} = G\gamma, \quad (2.11)$$

and the physical metric takes the form

$$ds^2 = -N^2 dt^2 + \frac{p_b^2}{L_0^2 p_c} dx^2 + p_c (d\theta^2 + \sin^2 \theta d\phi^2). \quad (2.12)$$

By comparing this metric with (2.2), and assuming we are working in Schwarzschild coordinates, we can see that

$$\frac{p_b^2}{L_0^2 p_c} = \left(\frac{2GM}{t} - 1 \right), \quad |p_c| = t^2. \quad (2.13)$$

This means that

$$p_b = 0, \quad p_c = 4G^2 M^2, \quad \text{On the horizon } t = 2GM \ (\tau = GM\pi), \quad (2.14)$$

$$p_b \rightarrow 0, \quad p_c \rightarrow 0, \quad \text{At singularity } t = 0 \ (\tau = 0), \quad (2.15)$$

where t is the time in Schwarzschild coordinates, and we have used the Schwarzschild lapse $N = \left(\frac{2GM}{t} - 1 \right)^{-\frac{1}{2}}$ to find the corresponding proper times $\tau = \int N dt \in (0, GM\pi)$.

Although the redefinitions (2.10), transform the metric such that it remains invariant under coordinate rescaling $r \rightarrow \xi r$, there still exists a freedom in rescaling the length of the interval \mathcal{I} itself by $L_0 \rightarrow \xi L_0$. This freedom manifests itself in transformation of the canonical variables in the following way

$$c \rightarrow c' = \xi c \quad p_c \rightarrow p'_c = p_c, \quad (2.16)$$

$$b \rightarrow b' = b \quad p_b \rightarrow p'_b = \xi p_b. \quad (2.17)$$

Note that here [6], since r_0 is chosen to be a physical scale, not an auxiliary one, there is no freedom associated with its rescaling, unlike the case in [3].

III. THE QUANTUM HAMILTONIAN CONSTRAINT

The next step is to find the classical Hamiltonian in loop variables, and then representing it as an operator on a suitable kinematical Hilbert space. We only briefly go over this, details can be found in previous works [3, 7]. Since in this model, the diffeomorphism constraint is trivially satisfied, after imposing the Gauss constraint, one is left only with the classical Hamiltonian constraint

$$C = - \int d^3x \frac{N}{\sqrt{|\det E|}} \epsilon_{ijk} E^{ai} E^{bj} \left(\frac{1}{\gamma^2} {}^0F_{ab}^k - \Omega_{ab}^k \right). \quad (3.1)$$

Here the integral is over the fiducial volume, and Ω_{ab}^k and ${}^0F_{ab}^k$ are the curvatures of the spin connection Γ_a^i , and the extrinsic curvature $K_a^i = \frac{1}{\gamma} (A_a^i - \Gamma_a^i)$, respectively. Since in loop quantum gravity the configuration variables are holonomies, not the connections themselves, these curvatures should be written in terms of them. In general, the holonomy of a connection A_a^i over edge e is the path ordered exponential

$$h_e[A] = \mathcal{P}\exp \left(\int_e A_a^i \tau_i dx^a \right). \quad (3.2)$$

In case of the present model, there are two types of holonomies: the one that is integrated over a path (or edge) λ , in the r direction,

$$h_r^{(\lambda)} = \cos \left(\frac{\lambda c}{2} \right) + 2\tau_3 \sin \left(\frac{\lambda c}{2} \right) \quad (3.3)$$

and the ones that are over edges μ , in θ and ϕ directions,

$$h_\theta^{(\mu)} = \cos \left(\frac{\mu b}{2} \right) + 2\tau_2 \sin \left(\frac{\mu b}{2} \right), \quad (3.4)$$

$$h_\phi^{(\mu)} = \cos \left(\frac{\mu b}{2} \right) - 2\tau_1 \sin \left(\frac{\mu b}{2} \right). \quad (3.5)$$

To find the curvature, one considers loops in $r - \theta$, $r - \phi$ and $\theta - \phi$ planes, such that the edges along the r direction in \mathbb{R} have a length $\delta_c \ell_c$ where $\ell_c = L_0$, and the edges along the longitude and the equator of \mathbb{S}^2 have length $\delta_b \ell_b$ where $\ell_b = r_0$. These lengths $\delta_b \ell_b, \delta_c \ell_c$ are considered with respect to the fiducial metric

$$ds_0^2 := dr^2 + r_0^2 (d\theta^2 + \sin^2 \theta d\phi^2). \quad (3.6)$$

Then the curvature ${}^0F_{ab}^k$ can be computed in terms of holonomies as

$${}^0F_{ab}^k = -2 \lim_{\text{Ar}\square \rightarrow 0} \text{Tr} \left(\frac{h_{\square ij}^{(\delta_{(i)}, \delta_{(j)})} - 1}{\delta_{(i)} \ell_{(i)} \delta_{(j)} \ell_{(j)}} \tau^k \right) {}^0E_a^{i0} E_b^j, \quad (3.7)$$

in which

$$h_{\square ij}^{(\delta_{(i)}, \delta_{(j)})} = h_i^{(\delta_{(i)})} h_j^{(\delta_{(j)})} \left(h_i^{(\delta_{(i)})} \right)^{-1} \left(h_j^{(\delta_{(j)})} \right)^{-1}. \quad (3.8)$$

Here $\delta_{(i)}$ correspond to δ_b or δ_c , $\ell_{(i)}$ correspond to $\ell_{(b)}$ or $\ell_{(c)}$, \square_{ij} is the loop with edges i, j , and $\text{Ar}\square$ is the area of the loop over which the curvature is being computed, and its limit to zero has been taken. Note, however, that in the quantum regime, due to the discreteness of the area, the loops can only be shrunk to a minimum value of $\Delta = \zeta \ell_{\text{Pl}}^2$ with $\zeta \approx \mathcal{O}(1)$ [3]. The choice in [6] is such that

$$\delta_b = \frac{\sqrt{\Delta}}{r_0}, \quad \delta_c = \frac{\sqrt{\Delta}}{L_0}. \quad (3.9)$$

As for the factor outside the parenthesis in (3.1), which contains the inverse triad, we rewrite it using Thiemann's trick

$$\frac{\epsilon_{ijk}}{\sqrt{|\det E|}} E^{aj} E^{bk} = \sum_k \frac{{}^0\epsilon^{abc} {}^0 E_c^k}{2\pi\gamma G \delta_{(k)} \ell_{(k)}} \text{Tr} \left(h_k^{(\delta_{(k)})} \left\{ \left(h_k^{(\delta_{(k)})} \right)^{-1}, V \right\} \tau_i \right), \quad (3.10)$$

in which V , the physical volume of the fiducial cell, is

$$V = \int d^3x \sqrt{\det q} = 4\pi |p_b| |p_c|^{1/2}. \quad (3.11)$$

The reason for writing the left hand side of 3.10 in the rather complicated form of its right hand side is the problem with representing the complicated expression $\frac{1}{\sqrt{|\det E|}}$, which contains a fraction as well as a square root. Hence one uses the Thiemann's trick by writing it as a Poisson bracket, that can then be turned into a bracket in quantization procedure using the Dirac prescription $\{A, B\} \rightarrow i [\hat{A}, \hat{B}]$ where no complication will arise and the issue is bypassed. Another more technical and more important reason is that the (discrete) spectrum of the area operator in loop quantum gravity includes 0 and thus the inverse operator is not properly defined on eigenstates with vanishing area. In summary, Thiemann's trick helps us hide the non-polynomiality of the theory and obtain a finite Hamiltonian.

Considering that Ω_{ab}^k in this case becomes

$$\Omega = -\sin(\theta) \tau^3 d\theta \wedge d\phi \quad (3.12)$$

and using (3.7), (3.10) and (3.11) in (3.1), we get

$$C = NC^{(\delta_b, \delta_c)} = -\frac{2N}{\gamma^3 G \delta_b^2 \delta_c} \left[2\gamma^2 \delta_b^2 \text{Tr} \left(\tau_3 h_x^{(\delta_c)} \left\{ \left(h_x^{(\delta_c)} \right)^{-1}, V \right\} \right) + \sum_{ijk} \epsilon^{ijk} \text{Tr} \left(h_{\square_{ij}}^{(\delta_{(i)}, \delta_{(j)})} h_k^{(\delta_{(k)})} \left\{ \left(h_k^{(\delta_{(k)})} \right)^{-1}, V \right\} \right) \right]. \quad (3.13)$$

To construct the kinematical Hilbert space on which this Hamiltonian constraint is to be represented, one notes that the algebra generated by the holonomies (3.3)-(3.5), is the algebra of the almost periodic functions of the form $\exp(i(\mu b + \lambda c)/2)$. This algebra (for just b or c) is isomorphic to the algebra of the continuous functions on the Bohr compactification of \mathbb{R} . Thus the kinematical Hilbert space corresponding to this space of configurations turns out to be the Cauchy completion of the space of square integrable functions over the Bohr compactified \mathbb{R}^2 , together with its associated Haar measure $\mathcal{H}_{\text{kin}} = L^2(\mathbb{R}_{\text{Bohr}}^2, d^2\mu_{\text{Bohr}})$. The basis states of this space satisfy the relation

$$\langle \mu', \lambda' | \mu, \lambda \rangle = \delta_{\mu, \mu'} \delta_{\lambda, \lambda'}, \quad (3.14)$$

where on the right hand side we have Kronecker deltas instead of Dirac deltas. On this space, in the momentum basis, the basic variables are represented as

$$\widehat{e^{\frac{1}{2}i\delta_b b}}|\mu, \lambda\rangle = |\mu + \delta_b, \lambda\rangle, \quad \widehat{e^{\frac{1}{2}i\delta_c c}}|\mu, \lambda\rangle = |\mu, \lambda + \delta_c\rangle, \quad (3.15)$$

$$\hat{p}_b|\mu, \lambda\rangle = \frac{\gamma\ell_{\text{Pl}}^2}{2}\mu|\mu, \lambda\rangle, \quad \hat{p}_c|\mu, \lambda\rangle = \gamma\ell_{\text{Pl}}^2\lambda|\mu, \lambda\rangle. \quad (3.16)$$

This is the quantum mechanical polymer representation corresponding to the original classical variables, which is unitarily inequivalent to the Schrödinger representation, due to some of the operators not being weakly continuous in their parameters, and hence the representation not satisfying the weak continuity premise of the Stone-von Neumann theorem. Due to the lack of weak continuity, the operators \hat{b} and \hat{c} are not well-defined on \mathcal{H}_{kin} , and thus their corresponding infinitesimal transformations do not exist. The theory, thus, only contains their corresponding finite transformations due to the action of $\widehat{e^{\frac{1}{2}i\delta_b b}}$ and $\widehat{e^{\frac{1}{2}i\delta_c c}}$, which are not to be considered as the literal exponentiation of \hat{b} and \hat{c} . This finite transformation is evident from (3.15). These result in p_b and p_c (components of the triad E_i^a) being discrete in the sense that they can only change by a finite minimum value. This, in principle, is how this approach yields the quantization and discreteness of the geometry.

Using the above consideration, the Hamiltonian constraint (3.13), is represented as

$$\begin{aligned} \hat{C}^{(\delta_b, \delta_c)} = & \frac{32i}{\gamma^3 \delta_b^2 \delta_c \ell_{\text{Pl}}^2} \left\{ \left[\sin\left(\frac{\delta_b b}{2}\right) \cos\left(\frac{\delta_b b}{2}\right) \sin\left(\frac{\delta_c c}{2}\right) \cos\left(\frac{\delta_c c}{2}\right) \right] \right. \\ & \times \left[\sin\left(\frac{\delta_b b}{2}\right) \hat{V} \cos\left(\frac{\delta_b b}{2}\right) - \cos\left(\frac{\delta_b b}{2}\right) \hat{V} \sin\left(\frac{\delta_b b}{2}\right) \right] \\ & + \frac{1}{2} \left[\sin^2\left(\frac{\delta_b b}{2}\right) \cos^2\left(\frac{\delta_b b}{2}\right) + \frac{1}{4} \gamma^2 \delta_b^2 \right] \\ & \left. \times \left[\sin\left(\frac{\delta_c c}{2}\right) \hat{V} \cos\left(\frac{\delta_c c}{2}\right) - \cos\left(\frac{\delta_c c}{2}\right) \hat{V} \sin\left(\frac{\delta_c c}{2}\right) \right] \right\}, \quad (3.17) \end{aligned}$$

where \hat{V} is the quantum volume operator, which is the representation of the classical volume (3.11), on \mathcal{H}_{kin} . We will consider rather the symmetric version of the above operator $\hat{C}_{\text{S}}^{(\delta_b, \delta_c)} = \frac{1}{2} \left(\hat{C}^{(\delta_b, \delta_c)} + \hat{C}^{(\delta_b, \delta_c)\dagger} \right)$.

IV. PATH INTEGRAL ANALYSIS: EFFECTIVE HAMILTONIAN AND NEW FEATURES

To find the effective version of the constraint we employ path integration. For standard mechanical systems path integrals yield expressions for the matrix elements of the evolution operators. The original derivation by Feynman involved the canonical theory expressing the evolution by composing \mathcal{N} infinitesimal ones and inserting complete basis between these. Such discrete time path integral gets replaced by the continuum one in the limit $\mathcal{N} \rightarrow \infty$. For gravitational models we have two different, but equivalent, routes to follow [33] (See [18, 20] for the case of non gravitational models): the use of a relational or deparametrized time scheme in which a matter degree of freedom is used as a clock, or else consider a timeless scheme that may include matter. In the latter case there is no evolution operator

but a constraint and its solutions, and we consider this scheme next. The aim is to construct a path integral expression for the so called ‘‘extraction amplitude’’ [33]

$$A(\mu_f, \lambda_f; \mu_i, \lambda_i) = \int d\alpha \left\langle \mu_f, \lambda_f \left| e^{-i\alpha \hat{C}_S^{(\delta_b, \delta_c)}} \right| \mu_i, \lambda_i \right\rangle, \quad (4.1)$$

which is a Green function for the transformation between kinematical and physical states, those that are annihilated by the quantum Hamiltonian constraint,

$$|\Psi_{\text{phys}}\rangle = \int d\alpha e^{-i\alpha \hat{C}_S^{(\delta_b, \delta_c)}} |\Psi_{\text{kin}}\rangle \quad (4.2)$$

with $|\Psi_{\text{kin}}\rangle \in \mathcal{H}_{\text{kin}}$, namely

$$\Psi_{\text{phys}}(\mu, \lambda) = \sum_{\lambda', \mu'} A(\mu, \lambda; \mu', \lambda') \Psi_{\text{kin}}(\mu', \lambda'). \quad (4.3)$$

To find the path integral representation of this Green function, as usual, we employ the ‘‘time slicing’’ method [33], by dividing the fictitious unit time interval into \mathcal{N} sub-intervals each with length $\epsilon = \frac{1}{\mathcal{N}}$ such that $e^{-i\alpha \hat{C}_S^{(\delta_b, \delta_c)}} = e^{-it\hat{H}}$, $\hat{H} := \alpha \hat{C}_S^{(\delta_b, \delta_c)}$, $t = 1$, and hence

$$A(\mu_f, \lambda_f, \mu, \lambda_i) = \int d\alpha \left\langle \mu_f, \lambda_f \left| \underbrace{e^{-i\epsilon\alpha \hat{C}_S^{(\delta_b, \delta_c)}} \dots e^{-i\epsilon\alpha \hat{C}_S^{(\delta_b, \delta_c)}}}_{\mathcal{N} \text{ times}} \right| \mu_i, \lambda_i \right\rangle. \quad (4.4)$$

By inserting $\hat{\mathbb{I}} = \sum_{(\mu, \lambda) \in \Gamma} |\mu, \lambda\rangle \langle \mu, \lambda|$, between the exponentials above, the amplitude is written as

$$A(\mu_f, \lambda_f, \mu, \lambda_i) = \int d\alpha \prod_{n=1}^{\mathcal{N}} \sum_{\mu_n, \lambda_n \in \gamma} \left\langle \mu_n, \lambda_n \left| e^{-i\epsilon\alpha \hat{C}_S^{(\delta_b, \delta_c)}} \right| \mu_{n-1}, \lambda_{n-1} \right\rangle, \quad (4.5)$$

where $\mu_{\mathcal{N}}, \lambda_{\mathcal{N}}, \mu_0, \lambda_0$ correspond to $\mu_f, \lambda_f, \mu_i, \lambda_i$ respectively. Each ‘‘short-time’’ amplitude can be expanded up to first order in ϵ as

$$\begin{aligned} \left\langle \mu_n, \lambda_n \left| e^{-i\epsilon\alpha \hat{C}_S^{(\delta_b, \delta_c)}} \right| \mu_{n-1}, \lambda_{n-1} \right\rangle &= \delta_{\mu_n, \mu_{n-1}} \delta_{\lambda_n, \lambda_{n-1}} - i\epsilon \left\langle \mu_n, \lambda_n \left| \hat{C}_S^{(\delta_b, \delta_c)} \right| \mu_{n-1}, \lambda_{n-1} \right\rangle + \mathcal{O}(\epsilon^2), \\ &= \left(\frac{1}{2\pi} \right)^2 \int_{-\pi/p_b^0}^{\pi/p_b^0} db_n \int_{-\pi/p_c^0}^{\pi/p_c^0} dc_n e^{-ib_n(p_n^b - p_{n-1}^b) - ic_n(p_n^c - p_{n-1}^c)} \\ &\quad - i\epsilon\alpha \left\langle \mu_n, \lambda_n \left| \hat{C}_S^{(\delta_b, \delta_c)} \right| \mu_{n-1}, \lambda_{n-1} \right\rangle + \mathcal{O}(\epsilon^2), \end{aligned} \quad (4.6)$$

where we have used $p_n^b = \frac{1}{2}\gamma\ell_{\text{Pl}}^2\mu_n$ and $p_n^c = \gamma\ell_{\text{Pl}}^2\lambda_n$.

To proceed, we need to compute the matrix element of the quantum Hamiltonian constraint $\hat{C}_S^{(\delta_b, \delta_c)}$. This turns out to be

$$\begin{aligned} \left\langle \mu', \lambda' \left| \hat{C}_S^{(\delta_b, \delta_c)} \right| \mu, \lambda \right\rangle &= -\frac{1}{\gamma^3 \delta_b^2 \delta_c \ell_{\text{Pl}}^2} [(V_{\mu+\delta_b, \lambda} - V_{\mu-\delta_b, \lambda}) \\ &\quad \times (\delta_{\mu', \mu+2\delta_b} - \delta_{\mu', \mu-2\delta_b}) (\delta_{\lambda', \lambda+2\delta_c} - \delta_{\lambda', \lambda-2\delta_c}) \\ &\quad + \frac{1}{2} (V_{\mu, \lambda+\delta_c} - V_{\mu, \lambda-\delta_c}) \delta_{\lambda', \lambda} \\ &\quad \times (\delta_{\mu', \mu+4\delta_b} - 2(1 + 2\delta_b^2 \gamma^2) \delta_{\mu', \mu} + \delta_{\mu', \mu-4\delta_b})], \end{aligned} \quad (4.7)$$

where $V_{\mu,\lambda}$ is the eigenvalue of the quantum volume operator \hat{V} in this basis. It is computed by using (3.16) to represent the classical volume (3.11), and then acting it on this basis,

$$\hat{V}|\mu, \lambda\rangle = V_{\mu,\lambda}|\mu, \lambda\rangle = 2\pi\gamma^{3/2}\ell_{\text{Pl}}^3|\mu||\lambda|^{1/2}|\mu, \lambda\rangle. \quad (4.8)$$

Using this, the matrix element (4.7) becomes

$$\begin{aligned} \langle \mu_n, \lambda_n | \hat{C}_S^{(\delta_b, \delta_c)} | \mu_{n-1}, \lambda_{n-1} \rangle &= \frac{2}{\gamma^3 \ell_{\text{Pl}}^2} \left(\frac{1}{2\pi} \right)^2 \int_{-\pi/p_b^0}^{\pi/p_b^0} db_n \int_{-\pi/p_c^0}^{\pi/p_c^0} dc_n \left\{ e^{-ib_n(p_n^b - p_{n-1}^b) - ic_n(p_n^c - p_{n-1}^c)} \right. \\ &\quad \times \left. \left[2V_1^{(n)} \frac{\sin(\delta_b b_n)}{\delta_b} \frac{\sin(\delta_c c_n)}{\delta_c} + V_2^{(n)} \left(\frac{\sin^2(\delta_b b_n)}{\delta_b^2} + \gamma^2 \right) \right] \right\}, \end{aligned} \quad (4.9)$$

where

$$\begin{aligned} V_2^{(n)} &:= \begin{cases} \pi\gamma^{3/2}\ell_{\text{Pl}}^3|\mu_n| \frac{(\lambda_n + \delta_c)^{1/2} - (\lambda_n - \delta_c)^{1/2}}{\delta_c} & \lambda_n \geq \delta_c \\ \pi\gamma^{3/2}\ell_{\text{Pl}}^3|\mu_n| \frac{(\lambda_n + \delta_c)^{1/2} - (\delta_c - \lambda_n)^{1/2}}{\delta_c} & |\lambda_n| < \delta_c \\ \pi\gamma^{3/2}\ell_{\text{Pl}}^3|\mu_n| \frac{(-\lambda_n - \delta_c)^{1/2} - (\delta_c - \lambda_n)^{1/2}}{\delta_c} & \lambda_n \leq -\delta_c \end{cases} \\ &= 4\pi\gamma\ell_{\text{Pl}}^2|p_n^b| \frac{\left(\sqrt{|p_n^c + p_c^0|} - \sqrt{|p_n^c - p_c^0|} \right)}{p_c^0}, \end{aligned} \quad (4.10)$$

and

$$\begin{aligned} V_1^{(n)} &:= \begin{cases} \pi\gamma^{3/2}\ell_{\text{Pl}}^3|\lambda_n|^{1/2} & \mu_n \geq \delta_b \\ \pi\gamma^{3/2}\ell_{\text{Pl}}^3|\lambda_n|^{1/2}\mu_n/\delta_b & |\mu_n| < \delta_b \\ -\pi\gamma^{3/2}\ell_{\text{Pl}}^3|\lambda_n|^{1/2} & \mu_n \leq -\delta_b \end{cases} \\ &= 4\pi\gamma\ell_{\text{Pl}}^2|p_n^c|^{\frac{1}{2}} \frac{|p_n^b + p_b^0| - |p_n^b - p_b^0|}{2p_b^0}, \end{aligned} \quad (4.11)$$

with

$$p_b^0 := \frac{1}{2}\gamma\ell_{\text{Pl}}^2\delta_b, \quad p_c^0 := \gamma\ell_{\text{Pl}}^2\delta_c. \quad (4.12)$$

Substituting all these back into the short-time amplitude (4.6) yields

$$\begin{aligned} \langle \mu_n, \lambda_n | e^{-i\epsilon\alpha\hat{C}_S^{(\delta_b, \delta_c)}} | \mu_{n-1}, \lambda_{n-1} \rangle &= \int_{-\pi/p_b^0}^{\pi/p_b^0} db_n \int_{-\pi/p_c^0}^{\pi/p_c^0} dc_n \left\{ e^{-ib_n(p_n^b - p_{n-1}^b) - ic_n(p_n^c - p_{n-1}^c)} \right. \\ &\quad \times \left. \left(1 - i\epsilon\alpha\tilde{C}(p_n^b, p_n^c, b_n, c_n) \right) \right\} + \mathcal{O}(\epsilon^2) \\ &= \int_{-\pi/p_b^0}^{\pi/p_b^0} db_n \int_{-\pi/p_c^0}^{\pi/p_c^0} dc_n \left\{ e^{-ib_n(p_n^b - p_{n-1}^b) - ic_n(p_n^c - p_{n-1}^c) - i\epsilon\alpha\tilde{C}(p_n^b, p_n^c, b_n, c_n)} \right\} \\ &\quad + \mathcal{O}(\epsilon^2), \end{aligned} \quad (4.13)$$

where

$$\tilde{C}(p_n^b, p_n^c, b_n, c_n) = \frac{2}{\gamma^3 \ell_{\text{Pl}}^2} \left[2V_1^{(n)} \frac{\sin(\delta_b b_n)}{\delta_b} \frac{\sin(\delta_c c_n)}{\delta_c} + V_2^{(n)} \left(\frac{\sin^2(\delta_b b_n)}{\delta_b^2} + \gamma^2 \right) \right]. \quad (4.14)$$

The amplitude (4.5), is the multiplication of these ‘short-time’ amplitudes,

$$A(\mu_f, \lambda_f, \mu, \lambda_i) = \int d\alpha \prod_{n=1}^{\mathcal{N}} \sum_{\mu_n, \lambda_n \in \Gamma} \int_{-\pi/p_b^0}^{\pi/p_b^0} db_n \int_{-\pi/p_c^0}^{\pi/p_c^0} dc_n \left\{ \exp \left(-i \left[\epsilon \sum_{n=1}^{\mathcal{N}} \frac{b_n (p_n^b - p_{n-1}^b) + c_n (p_n^c - p_{n-1}^c)}{\epsilon} + \epsilon \alpha \sum_{n=1}^{\mathcal{N}} \tilde{C}(p_n^b, p_n^c, b_n, c_n) \right] \right) \right\} + \mathcal{O}(\epsilon^2).$$

The first term in the exponential can be written as

$$\sum_{n=1}^{\mathcal{N}} b_n (p_n^b - p_{n-1}^b) + c_n (p_n^c - p_{n-1}^c) = \text{B.T.} - \sum_{n=1}^{\mathcal{N}-1} (b_{n+1} - b_n) p_n^b + (c_{n+1} - c_n) p_n^c, \quad (4.15)$$

where B.T. is the boundary term

$$\text{B.T.} = b_{\mathcal{N}} p_{\mathcal{N}}^b - b_1 p_0^b + c_{\mathcal{N}} p_{\mathcal{N}}^c - c_1 p_0^c. \quad (4.16)$$

Then, the amplitude becomes

$$A(\mu_f, \lambda_f, \mu, \lambda_i) = \int d\alpha \prod_{n=1}^{\mathcal{N}} \sum_{\mu_n, \lambda_n \in \Gamma} \int_{-\pi/p_b^0}^{\pi/p_b^0} db_n \int_{-\pi/p_c^0}^{\pi/p_c^0} dc_n \left\{ \exp \left(i \left[\epsilon \sum_{n=1}^{\mathcal{N}} \frac{b_{n+1} - b_n}{\epsilon} p_n^b + \frac{c_{n+1} - c_n}{\epsilon} p_n^c - \epsilon \alpha \sum_{n=1}^{\mathcal{N}} \tilde{C}(p_n^b, p_n^c, b_n, c_n) + \text{B.T.} \right] \right) \right\} + \mathcal{O}(\epsilon^2).$$

Finally taking the limit $\mathcal{N} \rightarrow \infty$ such that $\mathcal{N}\epsilon = 1$, we arrive at

$$A(\mu_f, \lambda_f, \mu, \lambda_i) = \int d\alpha \int Db \int Dc \exp \left\{ i \int_{t_i}^{t_f} dt \left[p_b \dot{b} + p_c \dot{c} - \alpha C_{\text{S-eff}}^{(\delta_b, \delta_c)}(p_b(t), p_c(t), b(t), c(t)) \right] + \underbrace{b_f p_f^b - b_i p_i^b + c_f p_f^c - c_i p_i^c}_{\text{B.T.}} \right\} \quad (4.17)$$

where in the limit taken, $\epsilon \sum_{n=1}^{\mathcal{N}-1} \rightarrow \int dt$, and $p_n^c, p_n^b \rightarrow p_c(t), p_b(t)$, respectively, and

$$\int Db \int Dc = \lim_{\mathcal{N} \rightarrow \infty} \prod_{n=1}^{\mathcal{N}} \sum_{\mu_n, \lambda_n \in \Gamma} \int_{-\pi/p_b^0}^{\pi/p_b^0} db_n \int_{-\pi/p_c^0}^{\pi/p_c^0} dc_n. \quad (4.18)$$

To transform the integrals from a bounded interval to the whole real line we use the Jacobi identity for periodic functions (Eq. (3.13) in [33]). From this, one can read off the effective Hamiltonian constraint from the path integral representation of the kernel as

$$C_{\text{S-eff}}^{(\delta_b, \delta_c)}(p_b, p_c, p_b, p_c) = -\frac{2}{\gamma^3 \ell_{\text{Pl}}^2} \left[2V_1(p_b, p_c) \frac{\sin(\delta_b b)}{\delta_b} \frac{\sin(\delta_c c)}{\delta_c} + V_2(p_b, p_c) \left(\frac{\sin^2(\delta_b b)}{\delta_b^2} + \gamma^2 \right) \right]. \quad (4.19)$$

Here

$$V_1(p_b, p_c) = \lim_{p_n^b, p_n^c \rightarrow p_b(t), p_c(t)} V_1^{(n)} = 4\pi\gamma\ell_{\text{Pl}}^2\beta_1(p_b, p_b^0) p_c^{\frac{1}{2}}, \quad (4.20)$$

with

$$\beta_1(p_b, p_b^0) = \frac{|p_b + p_b^0| - |p_b - p_b^0|}{2p_b^0}. \quad (4.21)$$

In the same manner

$$V_2(p_b, p_c) = \lim_{p_n^b, p_n^c \rightarrow p_b(t), p_c(t)} V_2^{(n)} = 4\pi\gamma\ell_{\text{Pl}}^2\beta_2(p_c, p_c^0) \frac{p_b}{p_c^{\frac{1}{2}}}, \quad (4.22)$$

in which

$$\beta_2(p_c, p_c^0) = p_c^{\frac{1}{2}} \frac{\left(\sqrt{|p_c + p_c^0|} - \sqrt{|p_c - p_c^0|}\right)}{p_c^0}. \quad (4.23)$$

Note that due to the form of p_c, p_c^0, p_b, p_b^0 , under a rescaling $L_0 \rightarrow \xi L_0$ we get

$$b \rightarrow b' = b \qquad c \rightarrow c' = \xi c \quad (4.24)$$

$$p_b \rightarrow p_b' = \xi p_b \qquad p_c \rightarrow p_c' = p_c \quad (4.25)$$

$$\delta_b = \frac{\sqrt{\Delta}}{r_0} \rightarrow \delta_b' = \delta_b \qquad \delta_c = \frac{\sqrt{\Delta}}{L_0} \rightarrow \delta_c' = \frac{\delta_c}{\xi} \quad (4.26)$$

$$\delta_b l_b = \delta_b r_0 \qquad \delta_c l_c = \delta_c L_0 \rightarrow \delta_c \xi L_0 \quad (4.27)$$

$$p_b^0 = \frac{1}{2}\gamma\ell_{\text{Pl}}^2\delta_b \rightarrow p_b^{0'} = p_b^0 \qquad p_c^0 = \gamma\ell_{\text{Pl}}^2\delta_c \rightarrow p_c^{0'} = \frac{p_c^0}{\xi} \quad (4.28)$$

Using these and the form of $\beta_1(p_b, p_b^0)$ and $\beta_2(p_c, p_c^0)$, we obtain the rescaling for these expressions as

$$\begin{aligned} \beta_1(p_b', p_b^{0'}) &= \frac{|p_b' + p_b^{0'}| - |p_b' - p_b^{0'}|}{2p_b^{0'}} \\ &= \frac{|\xi p_b + p_b^0| - |\xi p_b - p_b^0|}{2p_b^0}, \end{aligned} \quad (4.29)$$

and

$$\begin{aligned} \beta_2(p_c', p_c^{0'}) &= p_c'^{\frac{1}{2}} \frac{\left(\sqrt{|p_c' + p_c^{0'}|} - \sqrt{|p_c' - p_c^{0'}|}\right)}{p_c^{0'}} \\ &= p_c^{\frac{1}{2}} \frac{\left(\sqrt{|p_c + \frac{p_c^0}{\xi}|} - \sqrt{|p_c - \frac{p_c^0}{\xi}|}\right)}{\frac{p_c^0}{\xi}}, \end{aligned} \quad (4.30)$$

and hence neither of the functions β_1 and β_2 are invariant.

With introduction of β_1 and β_2 , the effective Hamiltonian (4.19) times the lapse function, $\frac{N}{16\pi G}$, is written as

$$\begin{aligned} C_{\text{S-eff}} &= \frac{N}{16\pi G} C_{\text{S-eff}}^{(\delta_b, \delta_c)} \\ &= -\frac{N}{2G\gamma^2} \left[2\beta_1(p_b, p_b^0) p_c^{\frac{1}{2}} \frac{\sin(\delta_b b)}{\delta_b} \frac{\sin(\delta_c c)}{\delta_c} + \beta_2(p_c, p_c^0) \frac{p_b}{p_c^{\frac{1}{2}}} \left(\frac{\sin^2(\delta_b b)}{\delta_b^2} + \gamma^2 \right) \right]. \end{aligned} \quad (4.31)$$

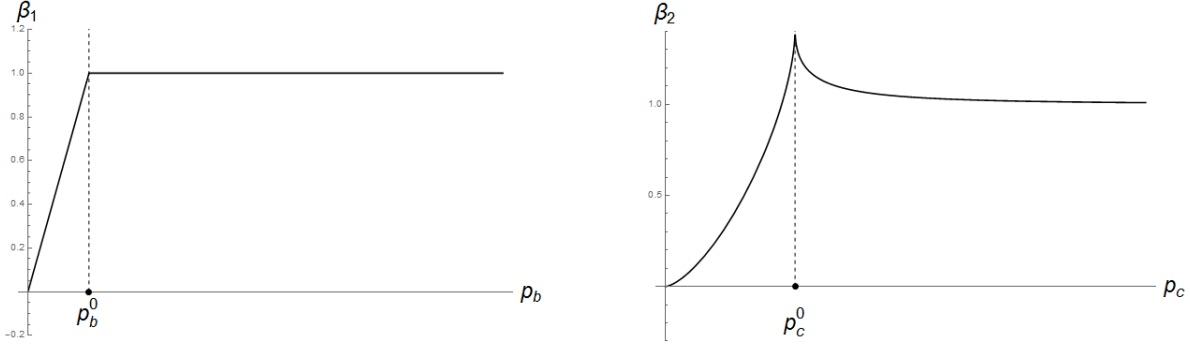


Figure 1. The functions β_1 and β_2 , with $p_b = 1 = p_c$. It is seen that for $p_b > p_b^0$ and $p_c \gg p_c^0$, they behave as $\beta_1, \beta_2 \rightarrow 1$.

This effective Hamiltonian resembles the ones that have been suggested in previous works, with the important difference of incorporating further inverse triad quantum corrections, encoded in functions β_1 and β_2 , as can be seen from (4.21) and (4.23). The profile of these functions are plotted in Fig. 1.

For a generic lapse function N , this effective Hamiltonian leads to the equations of motion, $\dot{F} = \{F, C_{S\text{-eff}}\}$, that read

$$\begin{aligned} \dot{b} = & -\frac{1}{2\gamma} \left[2\beta_1(p_b, p_b^0) p_c^{\frac{1}{2}} \frac{\sin(\delta_b b)}{\delta_b} \frac{\sin(\delta_c c)}{\delta_c} \{b, N\} \right. \\ & + \beta_2(p_c, p_c^0) \frac{1}{p_c^{\frac{1}{2}}} \left(\frac{\sin^2(\delta_b b)}{\delta_b^2} + \gamma^2 \right) (p_b \{b, N\} + N(p_b)) \\ & \left. + 2N \frac{\partial \beta_1(p_b, p_b^0)}{\partial p_b} p_c^{\frac{1}{2}} \frac{\sin(\delta_b b)}{\delta_b} \frac{\sin(\delta_c c)}{\delta_c} \right], \end{aligned} \quad (4.32)$$

$$\begin{aligned} \dot{c} = & -\frac{1}{\gamma} \left[\beta_1(p_b, p_b^0) p_c^{\frac{1}{2}} \frac{\sin(\delta_b b)}{\delta_b} \frac{\sin(\delta_c c)}{\delta_c} \left(2\{c, N\} + \frac{N}{p_c} \right) \right. \\ & \left. + \beta_2(p_c, p_c^0) \frac{p_b}{p_c^{\frac{1}{2}}} \left(\{c, N\} - \frac{N}{2p_c} \right) \left(\frac{\sin^2(\delta_b b)}{\delta_b^2} + \gamma^2 \right) + N \frac{p_b}{p_c^{\frac{1}{2}}} \frac{\partial \beta_2(p_c, p_c^0)}{\partial p_c} \left(\frac{\sin^2(\delta_b b)}{\delta_b^2} + \gamma^2 \right) \right], \end{aligned} \quad (4.33)$$

$$\begin{aligned} \dot{p}_b = & -\frac{1}{2\gamma} \left[2\beta_1(p_b, p_b^0) p_c^{\frac{1}{2}} \frac{\sin(\delta_c c)}{\delta_c} \left(\frac{\sin(\delta_b b)}{\delta_b} \{p_b, N\} - N \cos(\delta_b b) \right) \right. \\ & \left. + \beta_2(p_c, p_c^0) \frac{p_b}{p_c^{\frac{1}{2}}} \left(-2N \frac{\sin(\delta_b b)}{\delta_b} \cos(\delta_b b) + \left(\frac{\sin^2(\delta_b b)}{\delta_b^2} + \gamma^2 \right) \{p_b, N\} \right) \right], \end{aligned} \quad (4.34)$$

$$\begin{aligned} \dot{p}_c = & -\frac{1}{\gamma} \left[2\beta_1(p_b, p_b^0) p_c^{\frac{1}{2}} \frac{\sin(\delta_b b)}{\delta_b} \left(\frac{\sin(\delta_c c)}{\delta_c} \{p_c, N\} - N \cos(\delta_c c) \right) \right. \\ & \left. + \beta_2(p_c, p_c^0) \frac{p_b}{p_c^{\frac{1}{2}}} \left(\frac{\sin^2(\delta_b b)}{\delta_b^2} + \gamma^2 \right) \{p_c, N\} \right]. \end{aligned} \quad (4.35)$$

Note that although the derivative of β_i are not well-defined at the kink at p^0 , nevertheless given the existence of a minimal radius at bounce, $p = p^0$ will not happen and one can use the derivatives of β_i in the above equations safely.

These equations will help us clarify some of the differences of our results from the previous ones, in the next sections.

V. ISSUES RAISED BY THE NEW CORRECTIONS

As mentioned earlier, in this model, a number of differences arise due to the presence of further inverse triad corrections that we have managed to compute through the path integral method. To further highlight these differences, and also to be able to compare our results with some of the previous works, we need to specify a specific lapse N , which is needed to write the explicit equations of motion in a certain frame. One such choice takes us to the Hamiltonian in [6] in the limit of not considering these additional inverse triad quantum corrections, *i.e.* when $\beta_1, \beta_2 \rightarrow 1$, is

$$N^{(1)} = \frac{\gamma \delta_b p_c^{\frac{1}{2}}}{\sin(\delta_b b)}, \quad (5.1)$$

for which the effective Hamiltonian becomes

$$C_{\text{eff}}^1 = -\frac{1}{2G\gamma} \left[2\beta_1 (p_b, p_b^0) p_c \frac{\sin(\delta_c c)}{\delta_c} + \beta_2 (p_c, p_c^0) p_b \left(\frac{\sin(\delta_b b)}{\delta_b} + \gamma^2 \frac{\delta_b}{\sin(\delta_b b)} \right) \right]. \quad (5.2)$$

This lapse, which at the classical level is $N = \frac{\gamma \sqrt{p_c}}{b}$, is quite useful because it decouples the classical equations of motion for b and p_b from those of c and p_c , and hence simplifies many of the associated analyses. Thus, in order to be able to compare our effective results with their classical counter parts, we need to use the same lapse, now in its effective form where $b \rightarrow \sin(\delta_b b)/b$.

It is clearly seen that this Hamiltonian matches that in [6] except for the presence of additional inverse triad corrections β_1, β_2 , while they will match exactly for $\beta_1, \beta_2 \rightarrow 1$.

The equations of motion corresponding to this effective Hamiltonian can be derived by using the lapse (5.1) in the equations of motion (4.32)-(4.35) which yields

$$\dot{b} = -\frac{1}{2} \left[2p_c \frac{\sin(\delta_c c)}{\delta_c} \frac{\partial \beta_1(p_b, p_b^0)}{\partial p_b} + \beta_2 (p_c, p_c^0) p_b \left(\frac{\sin(\delta_b b)}{\delta_b} + \gamma^2 \frac{\delta_b}{\sin(\delta_b b)} \right) \right], \quad (5.3)$$

$$\dot{c} = -\left[2\beta_1 (p_b, p_b^0) \frac{\sin(\delta_c c)}{\delta_c} + p_b \frac{\partial \beta_2(p_c, p_c^0)}{\partial p_c} \left(\frac{\sin(\delta_b b)}{\delta_b} + \gamma^2 \frac{\delta_b}{\sin(\delta_b b)} \right) \right] \quad (5.4)$$

$$\dot{p}_b = \frac{1}{2} \beta_2 (p_c, p_c^0) p_b \cos(\delta_b b) \left(1 - \gamma^2 \frac{\delta_b^2}{\sin^2(\delta_b b)} \right), \quad (5.5)$$

$$\dot{p}_c = 2\beta_1 (p_b, p_b^0) p_c \cos(\delta_c c). \quad (5.6)$$

The lapse (5.1), however, is not the only choice for which the effective Hamiltonian will be the same as the Hamiltonian [6], in the limit $\beta_1, \beta_2 \rightarrow 1$. In fact any other lapse functions $N^{(2)}$, such that $\lim_{\beta_1, \beta_2 \rightarrow 1} N^{(1)} = \lim_{\beta_1, \beta_2 \rightarrow 1} N^{(2)}$, will do, for which $N^{(2)} = \frac{\gamma \delta_b \sqrt{p_c}}{\beta_2 \sin(\delta_b b)}$ is an example.

One of the differences due to the presence of the β_1, β_2 functions is related to the minimum value of p_c . In classical theory, at the horizon, $p_c = 4G^2 M^2$, and by approaching the singularity, $p_b \rightarrow 0$ and $p_c \rightarrow 0$, as stated in 2.15. But, in the effective theory, due to the

discreteness of the geometry, both of these functions bounce at the singularity and their minimum is related to the minimum length. In our model however, regardless of the lapse function, this minimum is different from what has been computed in previous works. To get this minimum value, we first note that

$$Q = \frac{\sin(\delta_c c)}{\delta_c} \frac{p_c}{\beta_2(p_c, p_c^0)}, \quad (5.7)$$

is a weak Dirac observable since

$$\dot{Q} = \left\{ Q, C_{\text{S-eff}}^{(\delta_b, \delta_c)} \right\} \approx \frac{2G\gamma \cos(\delta_c c) p_c}{\beta_2^2(p_c, p_c^0)} \frac{\partial \beta_2(p_c, p_c^0)}{\partial p_c} C_{\text{S-eff}}^{(\delta_b, \delta_c)} \approx 0. \quad (5.8)$$

On the other hand we can see from (5.6) that the extremum of p_c happens for $\cos(\delta_c c) = 0$ or $\sin(\delta_c c) = \pm 1$. Notice that we are not claiming $\sin(\delta_c c) = \pm 1$ leads to the minimum of Q . Rather, we are deducing a minimum value for p_c solely from (5.6) and independently of (5.7) without any reference to Q . Using the value $\sin(\delta_c c) = +1$ in (5.7) yields

$$p_{c(\min)} = Q \delta_c \beta_2(p_{c(\min)}, p_c^0). \quad (5.9)$$

After solving for $p_{c(\min)}$ and using (4.12), one finds the minimum value to be

$$p_{c(\min)} = \frac{Q \Delta^{\frac{1}{2}}}{L_0} \frac{1}{\sqrt{1 - \left(\frac{\gamma \ell_{\text{P1}}^2}{2Q}\right)^2}}, \quad p_c > p_c^0. \quad (5.10)$$

The weak Dirac observable similar to Q in [6] is $Q^{\text{C-S}} = \frac{\sin(\delta_c c)}{\delta_c} p_c$, which makes their minimum value $p_{c(\min)}^{\text{C-S}} = Q^{\text{C-S}} \delta_c$. The value of the constant of motion Q can be determined by the initial conditions of the equations of motion. In [6] the initial conditions for the equations of motion are identified such that when solving, they lead directly to the Schwarzschild metric. We use the same initial values as [6], so that in the classical limit we directly obtain the Schwarzschild metric. Hence, if in the above equation, we take Q equal to the constant of motion in [6] $Q^{\text{C-S}} = \gamma L_0 GM$, we will get

$$p_{c(\min)} = \gamma GM \sqrt{\Delta} \frac{1}{\sqrt{1 - \left(\frac{\ell_{\text{P1}}^2}{2GML_0}\right)^2}}, \quad p_c > p_c^0. \quad (5.11)$$

This is the value of the p_c at time of the bounce, and has a pure quantum origin such that for $G\hbar \rightarrow 0$, one gets $\Delta \rightarrow 0$ and thus $p_{c(\min)} \rightarrow 0$. Clearly this new value for minimum of p_c is different from what computed in [6] by a factor of $\frac{1}{\sqrt{1 - \frac{1}{4} \left(\frac{\ell_{\text{P1}}^2}{GML_0}\right)^2}}$, but, it depends on

the auxiliary parameter L_0 . This dependence on L_0 or its rescaling $L_0 \rightarrow \xi L_0$, shows itself in several places. Let us consider for instance a congruence of geodesic observers and their corresponding shear and expansion. Their dependence upon L_0 is an undesirable effect, since the physical results should not depend on an auxiliary variable or its rescaling. This can be traced back to the presence of the new corrections β_1 and β_2 . To see this in a more concrete way, we first consider the expansion θ . For a generic lapse it can be written as

$$\theta = \frac{\dot{p}_b}{N p_b} + \frac{\dot{p}_c}{2N p_c}, \quad (5.12)$$

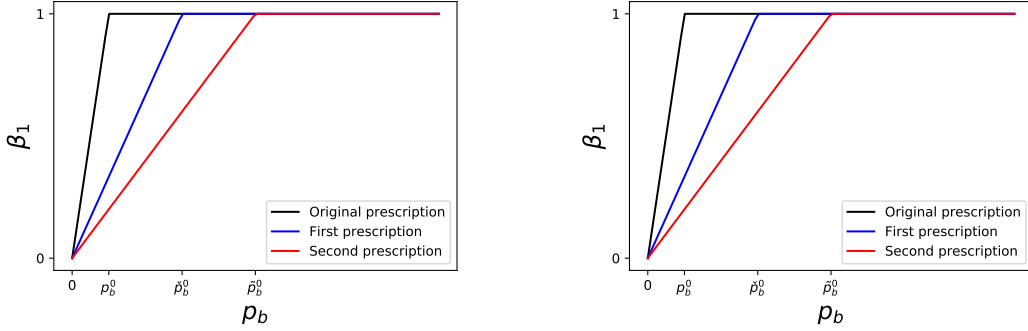


Figure 2. Comparison of the the original β_1, β_2 with the new functions $\tilde{\beta}_1, \tilde{\beta}_2$ of the first prescription and $\check{\beta}_1, \check{\beta}_2$ of the second prescription.

which for $N = 1$ (and on constraint surface) turns out to be

$$\theta = \frac{1}{\gamma} \left\{ \beta_1(p_b, p_b^0) p_c^{\frac{1}{2}} \left[\frac{\sin(\delta_c c) \cos(\delta_b b)}{p_b \delta_c} + \frac{\sin(\delta_b b) \cos(\delta_c c)}{p_c \delta_b} \right] + \beta_2(p_c, p_c^0) \frac{1}{p_c^{\frac{1}{2}}} \frac{\sin(\delta_b b) \cos(\delta_b b)}{\delta_b} \right\}. \quad (5.13)$$

From the transformation properties of the objects involved, it can be seen that although all the combination $\delta_b b, \delta_c c, p_b \delta_c, p_c \delta_b$ in the terms above are invariant under a rescaling $L_0 \rightarrow \xi L_0$, the expansion θ itself is not, precisely because the presence and noninvariance of $\beta_1(p_b, p_b^0)$ and $\beta_2(p_c, p_c^0)$.

We can also compute shear σ^2

$$\sigma^2 = \frac{1}{3} \left(-\frac{\dot{p}_b}{N p_b} + \frac{\dot{p}_c}{N p_c} \right)^2 \quad (5.14)$$

to see that for $N = 1$ we get

$$\sigma^2 = \frac{1}{3\gamma^2} \left\{ \beta_1(p_b, p_b^0) p_c^{\frac{1}{2}} \left[2 \frac{\sin(\delta_b b) \cos(\delta_c c)}{p_c \delta_b} - \frac{\sin(\delta_c c) \cos(\delta_b b)}{p_b \delta_c} \right] - \beta_2(p_c, p_c^0) \frac{(p_b)}{p_c^{\frac{1}{2}}} \frac{\sin(\delta_b b) \cos(\delta_b b)}{\delta_b} \right\}^2. \quad (5.15)$$

Again in the terms above, the only noninvariant parts under rescalings are $\beta_1(p_b, p_b^0)$ and $\beta_2(p_c, p_c^0)$ as was discussed in Eqs. (4.29) and (4.30). Thus a strong hint is that a solution that renders both β_1 and β_2 , invariant under rescalings, will resolve all of the above issues. Finding such a solution is the subject of the next section.

VI. PROPOSALS TO DEAL WITH THE ISSUES

The above observations together with the detailed forms of β_1 and β_2 , suggest that some sort of interchanging $p_b^0 \leftrightarrow p_c^0$ can fix the problem, either just in β_2 , or in both β_1 and β_2 .

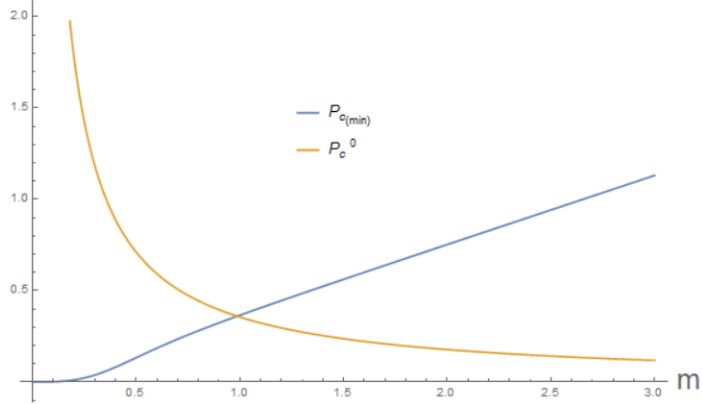


Figure 3. The effects of the corrections are relevant when $p_{c(\min)}$ is comparable to, or smaller than p_c^0 . In our proposal, this happens for $M_B \approx M_{P1}$.

At a first glance, it seems that this can be achieved by interchanging $\delta_b \leftrightarrow \delta_c$, but this has two problems: it is not clear if there are restrictions in doing so, and more importantly, although it fixes the invariance problem in β_2 , it makes almost every other terms in θ and σ^2 noninvariant. So we should find a way of interchanging $\delta_b \leftrightarrow \delta_c$ that only results in an interchange $p_b^0 \leftrightarrow p_c^0$, but does not lead to any modifications or interchange of $\delta_b \leftrightarrow \delta_c$ outside p_b^0 and p_c^0 . In other words, it should only affect triad corrections but not the holonomy ones. By looking at (3.1), (3.7), and (3.10), we notice that this can be achieved by some sort of interchange of δ_b and δ_c but just in the Thiemann's formula (3.10) (which is allowed classically), and not in the computations of the curvature in (3.7). Given this observation, we make two proposals which work particularly well at or near the singularity, and are explained in the following sections.

A. Proposal one: $\delta_b \leftrightarrow \delta_c$ in Thiemann's formula

The first proposal is to mutually interchange, r_0 and L_0 in δ_b, δ_c amounting to the exchange $\delta_b \leftrightarrow \delta_c$ only in Thiemann's formula (3.10) which can always be done classically. This only affects the inverse triad correction by essentially interchanging $p_b^0 \leftrightarrow \frac{1}{2}p_c^0$, while not altering the terms that depend on holonomy corrections. Consequently δ_b and δ_c remain the same whenever they appear outside p_b^0 or p_c^0 . As we will see, this has several desired consequences. After such an interchange $\delta_b \leftrightarrow \delta_c$, the quantities p_b^0, p_c^0, β_1 and β_2 are replaced by their new versions denoted by a tilde as

$$\tilde{p}_b^0 = \frac{1}{2}\gamma\ell_{P1}^2\delta_c = \frac{1}{2}p_c^0, \quad (6.1)$$

$$\tilde{p}_c^0 = \gamma\ell_{P1}^2\delta_b = 2p_b^0, \quad (6.2)$$

$$\tilde{\beta}_1(p_b, \tilde{p}_b^0) = \frac{|p_b + \tilde{p}_b^0| - |p_b - \tilde{p}_b^0|}{2\tilde{p}_b^0}, \quad (6.3)$$

$$\tilde{\beta}_2(p_c, \tilde{p}_c^0) = p_c^{\frac{1}{2}} \frac{\left(\sqrt{|p_c + \tilde{p}_c^0|} - \sqrt{|p_c - \tilde{p}_c^0|}\right)}{\tilde{p}_c^0}. \quad (6.4)$$

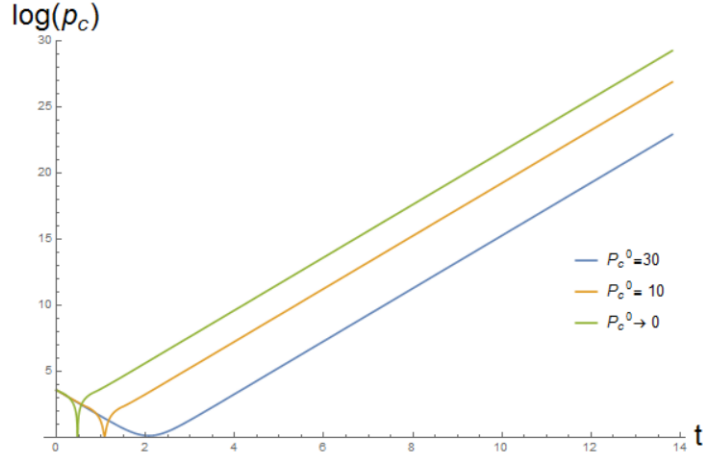


Figure 4. Effects of the inverse triad corrections on the evolution of $p_c(t)$ for distinct values of p_c^0 . The starting point of the curves corresponds to the same black hole mass, while the end of them is associated to the white hole mass as indicated in Eq. (6.10). Here we have considered a black hole with mass 2 in Planck units, $L_0 = 10$ and $\gamma = .2375$. These graphs were produced by numerically solving the equations of motion in Python using the Runge–Kutta method of fourth order. The initial and final times are determined by the condition $p_b(t_i) = p_b(t_f) = 0$ numerically. The black hole horizon is at $p_c(t_i)$ and the white horizon at $p_c(t_f)$ where in this plot $t_f \approx 14$.

The profile of these new function $\tilde{\beta}_1, \tilde{\beta}_2$ in comparison with the original β_1, β_2 and the new function from the second prescription $\tilde{\beta}_1, \tilde{\beta}_2$ (see next section) can be seen in Fig. 2. Considering (3.9), we see that under a rescaling $L_0 \rightarrow \xi L_0$, one gets

$$\tilde{p}_b^0 \rightarrow \tilde{p}_b^{0'} = \frac{\tilde{p}_b^0}{\xi}, \quad (6.5)$$

$$\tilde{p}_c^0 \rightarrow \tilde{p}_c^{0'} = \tilde{p}_c^0, \quad (6.6)$$

$$\tilde{\beta}_1(p_b, \tilde{p}_b^0) \rightarrow \tilde{\beta}_1'(p_b', \tilde{p}_b^{0'}) = \tilde{\beta}_1\left(p_b, \frac{\tilde{p}_b^0}{\xi^2}\right), \quad (6.7)$$

$$\tilde{\beta}_2(p_c, \tilde{p}_c^0) \rightarrow \tilde{\beta}_2'(p_c', \tilde{p}_c^{0'}) = \tilde{\beta}_2(p_c, \tilde{p}_c^0). \quad (6.8)$$

It is seen that now $\tilde{\beta}_2$ is invariant under rescalings while $\tilde{\beta}_1$ is not. Looking at (2.14) and (2.15) and the form of $\tilde{\beta}$'s, we notice that since $\tilde{\beta}_1$ becomes important for small p_b (also see Fig. 1), it modifies the behavior near the horizon, while β_2 is important for the modifications near the singularity because it becomes different from unity for small p_c .

However, for $p_b < \tilde{p}_b^0$ where $\tilde{\beta}_1$ becomes important, it will depend on the rescaling. This means that the classical behavior at the horizon will be affected in this way. But, if one assumes that one can consider $L_0 \rightarrow \infty$ at the end, this modification will be avoided (because the region of $p_b < \tilde{p}_b^0$ disappears and we only have $p_b > 0$ for which $\tilde{\beta}_1 \rightarrow 1$ and obviously invariant, see (6.3)). Furthermore the quantum corrections at the singularity will not be modified, since for this limit, $\tilde{\beta}_2$ is unaffected. This limit can be taken for a genuine cosmological model and here we will assume that it is also valid for black holes.

The limit $L_0 \rightarrow \infty$ may also be considered for β terms in Sec V. From Eqs. (4.29) and (4.30), it can be seen that this limit eliminates the inverse triad effects of β_2 which is

responsible for corrections at or close to the bounce, since in that limit $\beta_2 \rightarrow 1$. But it does not remove the effects of β_1 which generates quantum correction at the horizon. Hence, it does not completely remove the dependency of the inverse triad corrections on fiducial quantities.

The first nice consequence of this prescription is that the minimum value of p_c which results in singularity avoidance is now independent of L_0 ,

$$p_{c(\min)} = \gamma GM \sqrt{\Delta} \frac{1}{\sqrt{1 - \left(\frac{\ell_{\text{pl}}}{2GM}\right)^4}}, \quad p_c > \tilde{p}_c^0 \quad (6.9)$$

while still retaining the factors of modification $\left(1 - \left(\frac{\ell_{\text{pl}}}{2GM}\right)^4\right)^{-\frac{1}{2}}$, which makes the the minimum for the bounce larger than the previous results. As is seen from the above expression and also from Fig. 3, this effect is important when $M \approx M_{\text{pl}}$. Furthermore, given this value of $p_{c(\min)}$, the curvature scalars are universally bounded.

Using the new tilde variables (6.1)-(6.4) to compute the expansion and shear, we get similar expression as in (5.13) and (5.15), but with replacing $\beta_1 \rightarrow \tilde{\beta}_1$, $\beta_2 \rightarrow \tilde{\beta}_2$, $p_b^0 \rightarrow \tilde{p}_b^0$ and $p_c^0 \rightarrow \tilde{p}_c^0$. As a result, all the terms inside the expressions for θ and σ^2 , that are proportional to $\tilde{\beta}_2$, not only become independent of L_0 , but also become invariant under its rescalings. On the other hand, the terms proportional to $\tilde{\beta}_1$, are not invariant under its rescalings. However, with our assumption $L_0 \rightarrow \infty$ for which $\tilde{\beta}_1 \rightarrow 1$, the latter issue is bypassed. Furthermore, the values of θ and σ^2 for $N = 1$ now remain finite at both the singularity and the horizon, given that at the horizon, $\tilde{\beta}_1 \rightarrow 0$, and $\tilde{\beta}_2$ is finite but nonzero, and at the singularity $\tilde{\beta}_1, \tilde{\beta}_2 \rightarrow 0$. In addition, with $L_0 \rightarrow \infty$, they are both invariant.

Another observation is about the mass of the white hole. The behavior of p_c in time, depends on the size of the parameter \tilde{p}_c^0 , and particularly, as can be seen from Fig. 4, the larger the size of \tilde{p}_c^0 , the larger the later values of p_c . The mass of the black hole and white hole are

$$M_B = M = \frac{\sqrt{p_c(t_i)}}{2G}, \quad M_W = \frac{\sqrt{p_c(t_f)}}{2G}, \quad (6.10)$$

in which t_i and t_f are the initial and final times when black hole forms, and then when after bouncing back to the new white hole with its own Schwarzschild radius, respectively. Here we have used $p_c = r_{\text{Schw}}^2$ with r_{Schw} being the Schwarzschild radius of the black and white holes at these two moments in time. As can be seen from Fig. 4, M_W then depends on the value of \tilde{p}_c^0 and thus on $\tilde{\beta}_2$. It turns out then that $M_W(\beta_2 \neq 1) > M_W(\beta_2 \rightarrow 1)$. The effect of new correction on the relation between the black hole and white hole masses can be seen from the graph of $M_W(M_B)$ in Fig. 5.

B. Proposal two: $\delta_b \leftrightarrow 1/\delta_c$ in Thiemann's formula

The second proposal is to mutually interchange $\delta_b \leftrightarrow \frac{1}{\delta_c}$, restricted again to the Thiemann's formula (3.10). This leads to the quantities p_b^0 , p_c^0 , β_1 and β_2 being replaced by their

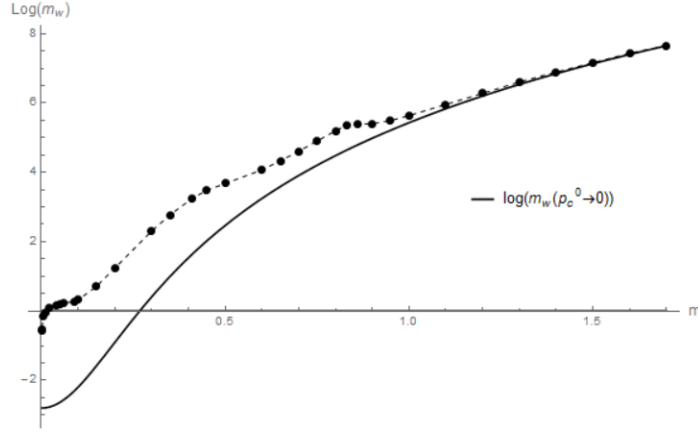


Figure 5. Comparing the behavior of $M_W (M_B)$ without inverse triad corrections (solid line) and the case with $\tilde{\beta}_2$ corrections.

new versions denoted by $\check{\sim}$ as

$$\check{p}_b^0 = \frac{1}{2} \frac{\gamma \ell_{\text{Pl}}^2}{\delta_c} = \frac{1}{2} \frac{\gamma^2 \ell_{\text{Pl}}^4}{p_c^0}, \quad (6.11)$$

$$\check{p}_c^0 = \frac{\gamma \ell_{\text{Pl}}^2}{\delta_b} = \frac{1}{2} \frac{\gamma^2 \ell_{\text{Pl}}^4}{p_b^0}, \quad (6.12)$$

$$\check{\beta}_1(p_b, \check{p}_b^0) = \frac{|p_b + \check{p}_b^0| - |p_b - \check{p}_b^0|}{2\check{p}_b^0}, \quad (6.13)$$

$$\check{\beta}_2(p_c, \check{p}_c^0) = p_c^{\frac{1}{2}} \frac{\left(\sqrt{|p_c + \check{p}_c^0|} - \sqrt{|p_c - \check{p}_c^0|} \right)}{\check{p}_c^0}. \quad (6.14)$$

In Fig. 2, the behavior of these new $\check{\beta}_1, \check{\beta}_2$ functions is compared to the original functions, and the functions from the first prescription. Interestingly, now both $\check{\beta}_1, \check{\beta}_2$ are invariant under rescalings. Thus, the effective behavior is independent of the auxiliary rescalings both on the horizon and at the singularity, and thus there is no need for the additional assumption $L_0 \rightarrow \infty$.

Let us see the effect of these prescription on $p_{c(\text{min})}$. Here again, a nice consequence of the prescription is that the minimum value of p_c is independent of L_0 ,

$$p_{c(\text{min})} = \gamma GM \sqrt{\Delta} \frac{1}{\sqrt{1 - \left(\frac{\ell_{\text{Pl}}^2}{\Delta} \right)^2}}, \quad p_c > \check{p}_c^0. \quad (6.15)$$

Compared to the previous works, this is now modified by a factor $\left(1 - \left(\frac{\ell_{\text{Pl}}^2}{\Delta} \right)^2 \right)^{-\frac{1}{2}}$, and unlike proposal one, this factor is now independent of the black hole mass, and instead depends on the ratio of the Planck area to the minimum area. These modifications are rather large for any black hole regardless of the mass. In any case, this value of $p_{c(\text{min})}$, means that in this case too, the curvature scalars are universally bounded. It is worth noting that, in this case, as expected, $p_{c(\text{min})} \rightarrow 0$ if $\Delta \rightarrow 0$, which is the case for a theory

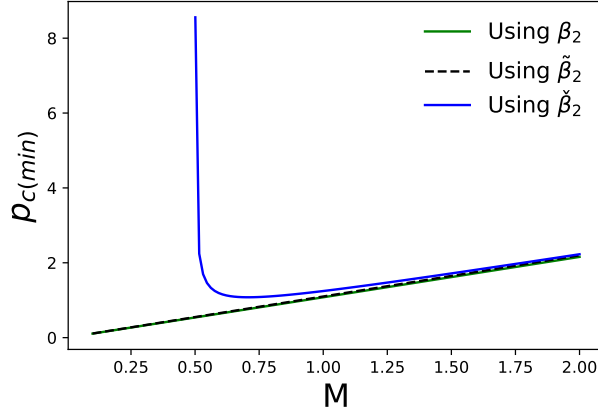


Figure 6. Dependence of $p_{c(\min)}$ on black hole mass M . The case without corrections denoted by C-S, is compared to the two prescriptions labeled by their corresponding β_2 functions. Although the lines for the second prescription and no-correction cases look the same, they have different slopes due to the modification factor $\left(1 - \left(\frac{\ell_{\text{Pl}}^2}{\Delta}\right)^2\right)^{-\frac{1}{2}}$ of the former case. The value of Δ used here is $\Delta = 4\sqrt{3}\pi\gamma\ell_{\text{Pl}}^2 \approx 5.17\ell_{\text{Pl}}^2$.

with a continuous spacetime. Fig. 6 compares the dependence of $p_{c(\min)}$ on black hole mass, M , for the two prescriptions as well as the case without the corrections.

The shear σ^2 and expansion θ have similar expression as in (5.13) and (5.15), but with replacing $\beta_1 \rightarrow \check{\beta}_1$, $\beta_2 \rightarrow \check{\beta}_2$, $p_b^0 \rightarrow \check{p}_b^0$ and $p_c^0 \rightarrow \check{p}_c^0$. Given that $\check{\beta}_1$ and $\check{\beta}_2$ are both invariant under rescalings, both θ and σ^2 are now fully invariant too, without the need for any further assumptions. Finally they both remain finite on both horizon and at the classical singularity since at the horizon, $\check{\beta}_1 \rightarrow 0$, and $\check{\beta}_2$ is finite but nonzero, and at the singularity $\check{\beta}_1, \check{\beta}_2 \rightarrow 0$.

Finally, the numerical evolution of p_c in time for the case without correction is compared to the second prescription in Fig. 7. It is seen that there is a horizontal asymptote corresponding to the case of second prescription, which gives a final value for the p_c which is smaller than the final value without corrections. In the case with no corrections, *i.e.*, in [6], the evolution of p_c stops at a finite time and the corresponding p_c is interpreted as the position of the horizon (the large dot in Fig. 7). In the presence of corrections and using the second proposal, however, p_c has an asymptotic behavior that depends on p_b^0 . Thus this asymptotic value may be interpreted as the horizon, although it is not reached at a finite time.

VII. DISCUSSION

The quest for a quantum theory of gravity involves looking for physical imprints of the merging of quantum and gravity effects in systems like black holes that classically exhibit singularities according to general relativity. In the case of Schwarzschild black hole, loop quantum gravity predicts the resolution of the classical singularity as well as a bouncing scenario connecting the black hole to a white hole, a phenomenon also predicted for some cosmological models, in such a case connecting a contracting with an expanding phase of the Cosmos. Previous research on the loop quantized black hole interior, either purely quantum

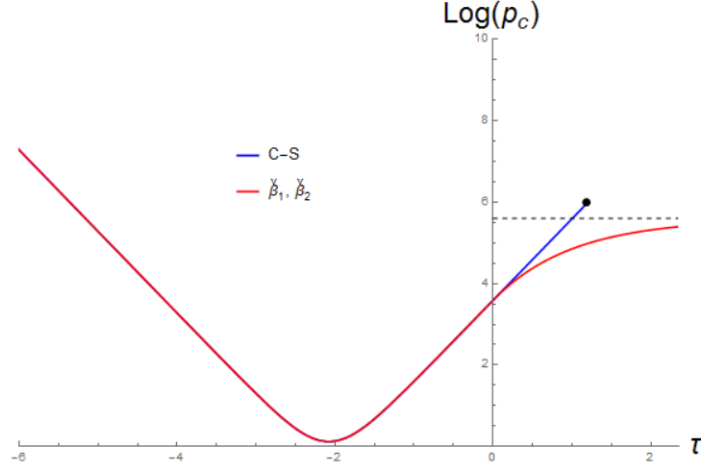


Figure 7. The evolution of p_c for the case without corrections denoted by C-S, versus the second prescriptions labeled by its corresponding $\check{\beta}_2$ functions. Note that the latter case has an asymptote.

[3] or effective [4–6, 14, 28, 29], shares this feature. However more insight has been obtained with the latter in that it allowed to investigate the physical independence from auxiliary parameters required in the formulation of the theory to further improve the description of the black to white hole bounce. Yet, all these works ignore the effects of the inverse triad corrections that enter the Hamiltonian constraint, basically to simplify the analysis.

In this work, we have extended and built up over the previous important works about the effective theory of the interior of the Schwarzschild modeled as a Kantowski-Sachs spacetime bouncing and with a resolved singularity. We started by using the proposal for the fiducial cell parameters in [6] to cope with the noncompact topology $\mathbb{R} \times \mathbb{S}^2$ of the model, and used a polymer path integral approach as systematic way to derive an effective Hamiltonian which automatically incorporates the inverse triad corrections. The effective Hamiltonian without these corrections resembles exactly the one in previous works. Although the inclusion of these corrections sheds more light on the physical nature of the problem, it raises some well-known issues in the analysis if one makes the usual choice of the parameters entering the model δ_b, δ_c in both curvature sector as well as in the inverse triad sector [6]. Such issues were the main reason they have been mostly ignored in previous works. These issues include the dependence of physical quantities like the expansion and shear on the rescaling of the fiducial parameter that is used to define the fiducial cell. Introduction of this cell is necessary to be able to compute the symplectic structure. In this case, the cell is a three dimensional cylinder whose height L_0 is the fiducial parameter, while its base is identified with a physical parameter, namely, the classical Schwarzschild radius. Furthermore, although the “minimum radius of black hole at bounce”, $p_{c(\min)}$, that we obtain here is different from the previous works, it also depends on the fiducial parameter L_0 and its rescalings, which thus renders the model physically unacceptable.

We tackle these issues by exploring the source of the dependence on the auxiliary parameters. It turns out that triad corrections, contained into two functions β_1 and β_2 , are both noninvariant under their rescalings. The first function β_1 is important for the behavior of the black hole at the horizon, while the second one, β_2 , is important for the behavior at or near the singularity. Looking more closely into the form of these correction functions, we see that some sort of interchanging of the parameters δ_b and δ_c , might resolve the issue;

recall these are used in the representation of the inverse triads in Thiemann’s formula, as well as in computing the curvatures. Further inspection reveals that if one only interchanges the parameters δ_b and δ_c in Thiemann’s formula, one could make β_1 and β_2 invariant, and furthermore, nothing in the computation of the curvature changes. In other words only the terms inside β_1 and β_2 are affected, which is the effect we are looking for.

Given this insight, we study two proposals. The first one consists of an interchange $\delta_b \leftrightarrow \delta_c$. As a first result, the minimum “radius” at the bounce $p_{c(\min)}$, now becomes independent of the auxiliary parameter and is modified because of the presence of the new corrections, such that its value is now larger than the value computed in previous works. This modification is particularly important when the mass of the black hole is comparable to the Planck’s mass. Furthermore, the function β_2 also becomes invariant. To investigate this case further, we consider a congruence of geodesic observers and show that the terms in the corresponding expansion θ and shear σ^2 proportional to β_2 are now also invariant. However, in this proposal, β_1 remains noninvariant. But the issues that correspond to this function not being invariant can be bypassed by assuming that at the end, one can take the limit $L_0 \rightarrow \infty$ which may be interpreted as the black hole being eternal. This limit is legitimate in cosmology but in a black hole setting, we should be more careful about its consequences. Using this limit, θ and σ^2 become both completely invariant under rescalings. This state of affairs can be improved as we next discuss it.

The second proposal amounts to the interchange $\delta_b \leftrightarrow 1/\delta_c$ in the original choice. It turns out in this case both β_1 and β_2 are invariant under rescalings without any need for additional assumptions such as $L_0 \rightarrow \infty$. As for the congruence of geodesic observers, both expansion θ and shear σ^2 now become fully (and not partially) invariant. Another new result with this proposal is that not only the minimum “radius” at the bounce $p_{c(\min)}$ is different, but now it does not depend on the mass of the black hole, but rather depends on the ratio of the minimum area to the Planck area, and is universal for all masses. This, in general, is certainly larger than what we derived from the previous proposal, particularly in cases where the mass of the black hole is much larger than the Planck’s mass.

Based on our results, one can see that due to the presence of β_1 , the classical behavior near the horizon will change due to quantum effects. Some of the other studies of black hole interior in loop quantum gravity have also found similar quantum effects at the horizon [34] [35], although without considering inverse triad corrections. Furthermore, in [36], and in some of the other scenarios such as the firewall proposal [37], these quantum effects near the horizon take a significant role. In our case, the correction term β_1 is responsible for any such quantum effects at the horizon. However, to fully understand and analyze the role and the impact of this correction on the modifications at the horizon we need to extend the model to describe both the interior and the exterior of the black hole. This is the subject of our future investigation.

Finally, we notice that the issue of mismatch between the masses of initial black hole M_B , and the final white hole M_W , worsens by introducing these new corrections such that $M_W(\beta_2 \neq 1) > M_W(\beta_2 \rightarrow 1)$. As mentioned before, this is due to the anisotropic nature of the Kantowski-Sachs model.

It is worth noting some of the recent works about the same subject. In [29] the authors expand the interior description to the full spacetime of the Schwarzschild black hole. However, a number of issues that arise in the asymptotic region in this model. The authors also do not consider the inverse triad corrections, although they put forward interesting results regarding the mass of large black holes (such as the relation between black and white holes).

They also consider a different prescriptions for δ_i parameters, so the effects of the inverse triad corrections will be different and need to be further studied. Also, based on our results, the inverse triad effects are reflected in the relation between the black and white hole masses even for small black holes. In this regards, in [29], one may need to include such inverse triad corrections to be able to correctly analyze small black holes. One can also analyze the black hole exterior in their model and check if there exist any significant quantum gravitational effect happening there.

In both [38] and [39], the authors do not start from a homogeneous space-time, so they do not resort to fiduciary parameters to define the dynamics, and the inverse triad corrections would not have a “rescaling” problems. Both works simplify the constraints before quantization by renaming variables and partial gauge fixing, so it is not clear how to implement the inverse triad corrections. Even so, [38] seeks to represent non-polynomial operators similar to the inverse triads, so one possibility is to introduce the inverse triad corrections by adapting the Thiemann trick. On the other hand, [39] simply does not consider these corrections arguing that in some cosmological cases they do not represent significant effects, but it is clear that this is not necessarily valid for other models. Given what we mentioned, it could be interesting to study the structure of inverse triad corrections in both of these works, since they would not depend on fiducial parameters, and to study possible effects in regions of interest. This will help expand what we know about these corrections so far.

Our results open the door to incorporating further quantum inverse triad corrections in works mentioned above and similar ones, as well as other quantum gravitational systems, hence providing a systematic method to deal with the issues raised by such corrections, which were mostly ignored in previous works.

ACKNOWLEDGMENTS

The authors would like to acknowledge the support from the CONACyT Grant No. 237351. S.R. would like to thank the CONACyT SNI support 59344. J.C.R. acknowledges the support of the grant from UAM. H.A.M.T. acknowledges the kind hospitality of the Physics department of the ESFM, IPN, during his sabbatical year

-
- [1] T. Thiemann, *Modern Canonical Quantum General Relativity*, Cambridge Monographs on Mathematical Physics (Cambridge University Press, 2007).
 - [2] C. Rovelli, *Quantum gravity*, Cambridge Monographs on Mathematical Physics (Univ. Pr., Cambridge, UK, 2004).
 - [3] A. Ashtekar and M. Bojowald, Quantum geometry and the Schwarzschild singularity, *Class. Quant. Grav.* **23**, 391 (2006), arXiv:gr-qc/0509075 [gr-qc].
 - [4] C. G. Boehmer and K. Vandersloot, Stability of the Schwarzschild Interior in Loop Quantum Gravity, *Phys. Rev.* **D78**, 067501 (2008), arXiv:0807.3042 [gr-qc].
 - [5] L. Modesto, Loop quantum black hole, *Class. Quant. Grav.* **23**, 5587 (2006), arXiv:gr-qc/0509078 [gr-qc].
 - [6] A. Corichi and P. Singh, Loop quantization of the schwarzschild interior revisited, *Class. Quant. Grav.* **33**, 055006 (2016), 1506.08015.

- [7] D. Cartin and G. Khanna, Wave functions for the Schwarzschild black hole interior, *Phys. Rev.* **D73**, 104009 (2006), arXiv:gr-qc/0602025 [gr-qc].
- [8] R. Gambini, J. Pullin, and S. Rastgoo, New variables for 1+1 dimensional gravity, *Class. Quant. Grav.* **27**, 025002 (2010), arXiv:0909.0459 [gr-qc].
- [9] S. Rastgoo, A local true Hamiltonian for the CGHS model in new variables, (2013), arXiv:1304.7836 [gr-qc].
- [10] A. Corichi, A. Karami, S. Rastgoo, and T. Vukašinac, Constraint Lie algebra and local physical Hamiltonian for a generic 2D dilatonic model, *Class. Quant. Grav.* **33**, 035011 (2016), arXiv:1508.03036 [gr-qc].
- [11] A. Corichi, J. Olmedo, and S. Rastgoo, Callan-Giddings-Harvey-Strominger vacuum in loop quantum gravity and singularity resolution, *Phys. Rev.* **D94**, 084050 (2016), arXiv:1608.06246 [gr-qc].
- [12] R. Gambini, J. Pullin, and S. Rastgoo, Quantum scalar field in quantum gravity: The vacuum in the spherically symmetric case, *Class. Quant. Grav.* **26**, 215011 (2009), arXiv:0906.1774 [gr-qc].
- [13] R. Gambini, J. Olmedo, and J. Pullin, Quantum black holes in Loop Quantum Gravity, *Class. Quant. Grav.* **31**, 095009 (2014), arXiv:1310.5996 [gr-qc].
- [14] J. Cortez, W. Cuervo, H. A. Morales-Técotl, and J. C. Ruelas, Effective loop quantum geometry of Schwarzschild interior, *Phys. Rev.* **D95**, 064041 (2017), arXiv:1704.03362 [gr-qc].
- [15] K. Blanchette, S. Das, S. Hergott, and S. Rastgoo, Black hole singularity resolution via the modified Raychaudhuri Equation in Loop Quantum Gravity, (2020), arXiv:2011.11815 [gr-qc].
- [16] R. Doran, F. S. N. Lobo, and P. Crawford, Interior of a Schwarzschild black hole revisited, *Found. Phys.* **38**, 160 (2008), arXiv:gr-qc/0609042 [gr-qc].
- [17] A. Ashtekar, S. Fairhurst, and J. L. Willis, Quantum gravity, shadow states, and quantum mechanics, *Class. Quant. Grav.* **20**, 1031 (2003), arXiv:gr-qc/0207106 [gr-qc].
- [18] H. A. Morales-Técotl, D. H. Orozco-Borunda, and S. Rastgoo, Polymer quantization and the saddle point approximation of partition functions, *Phys. Rev.* **D92**, 104029 (2015), arXiv:1507.08651 [gr-qc].
- [19] H. A. Morales-Técotl, D. H. Orozco-Borunda, and S. Rastgoo, Polymerization, the Problem of Access to the Saddle Point Approximation, and Thermodynamics, in *Proceedings, 14th Marcel Grossmann Meeting*, Vol. 4 (2017) pp. 4054–4059, arXiv:1603.08076 [gr-qc].
- [20] H. A. Morales-Técotl, S. Rastgoo, and J. C. Ruelas, Path integral polymer propagator of relativistic and nonrelativistic particles, *Phys. Rev.* **D95**, 065026 (2017), arXiv:1608.04498 [gr-qc].
- [21] A. Ashtekar and P. Singh, Loop Quantum Cosmology: A Status Report, *Class. Quant. Grav.* **28**, 213001 (2011), arXiv:1108.0893 [gr-qc].
- [22] A. Ashtekar, M. Bojowald, and J. Lewandowski, Mathematical structure of loop quantum cosmology, *Adv. Theor. Math. Phys.* **7**, 233 (2003), arXiv:gr-qc/0304074 [gr-qc].
- [23] A. Ashtekar, T. Pawłowski, and P. Singh, Quantum Nature of the Big Bang: An Analytical and Numerical Investigation. I., *Phys. Rev.* **D73**, 124038 (2006), arXiv:gr-qc/0604013 [gr-qc].
- [24] A. Ashtekar, T. Pawłowski, and P. Singh, Quantum nature of the big bang: Improved dynamics, *Phys. Rev.* **D74**, 084003 (2006), gr-qc/0607039.
- [25] J. Ben Achour, F. Lamy, H. Liu, and K. Noui, Polymer Schwarzschild black hole: An effective metric, *EPL* **123**, 20006 (2018), arXiv:1803.01152 [gr-qc].
- [26] M. Bojowald, S. Brahma, and D.-h. Yeom, Effective line elements and black-hole models in canonical loop quantum gravity, *Phys. Rev.* **D98**, 046015 (2018), arXiv:1803.01119 [gr-qc].

- [27] J. Olmedo, S. Saini, and P. Singh, From black holes to white holes: a quantum gravitational, symmetric bounce, *Class. Quant. Grav.* **34**, 225011 (2017), arXiv:1707.07333 [gr-qc].
- [28] A. Ashtekar, J. Olmedo, and P. Singh, Quantum Transfiguration of Kruskal Black Holes, *Phys. Rev. Lett.* **121**, 241301 (2018), arXiv:1806.00648 [gr-qc].
- [29] A. Ashtekar, J. Olmedo, and P. Singh, Quantum extension of the Kruskal spacetime, *Phys. Rev.* **D98**, 126003 (2018), arXiv:1806.02406 [gr-qc].
- [30] M. Assanioussi, A. Dapor, and K. Liegener, Perspectives on the dynamics in a loop quantum gravity effective description of black hole interiors, *Phys. Rev.* **D101**, 026002 (2020), arXiv:1908.05756 [gr-qc].
- [31] N. Bodendorfer, F. M. Mele, and J. Munch, Mass and Horizon Dirac Observables in Effective Models of Quantum Black-to-White Hole Transition, (2019), arXiv:1912.00774 [gr-qc].
- [32] D. Arruga, J. Ben Achour, and K. Noui, Deformed General Relativity and Quantum Black Holes Interior, (2019), arXiv:1912.02459 [gr-qc].
- [33] A. Ashtekar, M. Campiglia, and A. Henderson, Path Integrals and the WKB approximation in Loop Quantum Cosmology, *Phys. Rev.* **D82**, 124043 (2010), arXiv:1011.1024 [gr-qc].
- [34] C. G. Boehmer and K. Vandersloot, Loop Quantum Dynamics of the Schwarzschild Interior, *Phys. Rev. D* **76**, 104030 (2007), arXiv:0709.2129 [gr-qc].
- [35] D.-W. Chiou, Phenomenological loop quantum geometry of the Schwarzschild black hole, *Phys. Rev. D* **78**, 064040 (2008), arXiv:0807.0665 [gr-qc].
- [36] H. M. Haggard and C. Rovelli, Quantum-gravity effects outside the horizon spark black to white hole tunneling, *Phys. Rev. D* **92**, 104020 (2015), arXiv:1407.0989 [gr-qc].
- [37] A. Almheiri, D. Marolf, J. Polchinski, and J. Sully, Black Holes: Complementarity or Firewalls?, *JHEP* **02**, 062, arXiv:1207.3123 [hep-th].
- [38] R. Gambini, J. Olmedo, and J. Pullin, Spherically symmetric loop quantum gravity: analysis of improved dynamics, *Class. Quant. Grav.* **37**, 205012 (2020), arXiv:2006.01513 [gr-qc].
- [39] J. G. Kelly, R. Santacruz, and E. Wilson-Ewing, Effective loop quantum gravity framework for vacuum spherically symmetric space-times, (2020), arXiv:2006.09302 [gr-qc].